J. Astrophys. Astr. (2021)42:98
https://doi.org/10.1007/s12036-021-09768-6

A study of the passage of high-speed solar wind streams, their plasma/field properties and space weather effects of geomagnetic disturbances

SALMAN TARIQ[1,*], HASAN NAWAZ[2], FAZZAL QAYYUM[2] and ZIA UL-HAQ[2]

[1]Remote Sensing, GIS and Climatic Research Lab (National Center of GIS and Space Applications), Department of Space Science, University of the Punjab, Lahore, Pakistan.
[2]Remote Sensing, GIS and Climatic Research Lab (National Center of GIS and Space Applications), Centre for Remote Sensing, University of the Punjab, Lahore, Pakistan.
Corresponding author. E-mail: salmantariq_pu@yahoo.com

MS received 3 December 2020; accepted 9 April 2021

Abstract. This study investigated the geomagnetic disturbances and high-speed solar-wind streams (HSSs) during the period of solar storms emitted from coronal holes. The contemplated long-term HSS observations were taken from 1963 to 2016. On the basis of the intensity of geomagnetic activity, solar storms were divided into four groups: weak (-50 nT $< D_{st} < -30$ nT), moderate (-100 nT $< D_{st} < -50$ nT), intense (-200 nT $< D_{st} < -100$ nT) and superstorms ($D_{st} < -200$ nT). The relationship between solar plasma/field parameters and geomagnetic disturbances was also studied in the course of HSSs. For this purpose, statistical distributions and correlation analyses have been performed during the passage of HSSs causing geomagnetic disturbances on the individual stages. It was found that variations in the magnitude of the magnetic field B (nT) and V (km/s) relative to disturbance storm time (D_{st}) index occur oppositely. During intense and super solar storms, the Earth's magnetic field becomes very weak due to a decrease in the D_{st} index. The annual time-series analysis suggests that the D_{st} and K_p*10 index are of decreasing trends, whereas Bz (nT) and Ey (mV/m) have increasing trends during the study period. D_{st} best correlates with the $K_p * 10$ index with the highest value of correlation coefficient (R) to be observed as 0.54. The value of R is found to be 0.51 between D_{st} and B (nT) during the passage of HSSs.

Keywords. D_{st}—geomagnetic storm—plasma—HSSs.

1. Introduction

A geomagnetic storm is characterized by the minimum value of disturbance storm time index (D_{st} index), which is a measure of the solar energy penetrating the Earth's ionosphere (Zhang *et al.* 2006), below a certain value (Sugiura & Chapman 1960). The main level of magnetic storms is characterized by the decrement in the D_{st} index and the increment in ring current, and the recovery phase by the waning of the ring current and an increase in the D_{st} index because of several energetic particle's loss mechanisms (Adebesin *et al.* 2013). The D_{st} index shows the strength of the geomagnetic disturbance and solar winds that hit the Earth's ionosphere. Other indices are also used such as the K_p index, to determine the intensity of planetary magnetic activity (Gosling *et al.* 1991; Richardson 2018). Based on the strength of geomagnetic activity, geomagnetic storms are classified as weak, moderate, intense and superstorms (Loewe & Prolss 1997; Alves *et al.* 2006; Mustajab & Badruddin 2011, 2013, 2017).

Solar winds (stream of charged particles) are continuously emanating from coronal holes (CHs) (Parker 1963). Solar winds are highly variant in their density, speed and direction, and determine the shape of Earth's magnetosphere. The study of high-speed solar-wind streams (HSSs) (speed >400 km/s) is important to understand the Earth's magnetosphere and solar-wind coupling. Solar storms of different intensities (i.e., weak, moderate, intense and superstorms) cause technological issues, e.g., power outages, satellite damage, communication failure and global positioning system (GPS) problems, which are directly or

Published online: 11 August 2021

indirectly related to human life (Gonzalez *et al.* 1994; Bothmer & Zhukov 2007; McManus *et al.* 2011; Badruddin & Kumar 2015).

The slow evolution of CHs allows a precise prediction of HSSs (Garton *et al.* 2018). Many researchers have studied the characteristics of HSSs providing various definitions for them (Intriligator 1973). Previous studies have used remotely sensed solar-wind datasets to observe the HSSs (Lindblad *et al.* 1989; Verbanac *et al.* 2001; Maris & Maris 2005; Vršnak *et al.* 2017; Lei *et al.* 2008; Gupta & Badruddin 2010; Kumar & Badruddin 2014; Xystouris *et al.* 2014). Several features of HSSs influence the geomagnetic activity (Alves *et al.* 2006; Zhang *et al.* 2006; Badruddin & Falak 2016; Yermolaev *et al.* 2018); the cosmic ray intensity (Badruddin 1996; Gupta & Badruddin 2009; Kumar & Badruddin 2014; Badruddin & Kumar 2016), the temperature (Ogunjabi *et al.* 2014) and the pressure (Cho *et al.* 2012) have been studied in the past.

For a long time, solar storm sources and interplanetary consequences of geomagnetic disturbances have been investigated (Snyder *et al.* 1963; Arnoldy 1971; Akasofu 1983), but several aspects of interplanetary causes and sources of solar storms are not understood completely. So, by the availability of long-term space-based high-resolution plasma/field interplanetary observations, geomagnetic disturbances can be well understood by a detailed study. Therefore, the study of the behavior of HSSs during the period of solar storms helps us to understand the sources and physics of geomagnetic disturbances, and the ability to forecast them. In this study, the passage of HSSs from 1963 to 2016 has been investigated using solar wind and plasma/field interplanetary datasets.

2. Data and analysis

Solar winds having speeds between 400 and 800 km/s are considered as HSSs (Gupta & Badruddin 2010; Kumar & Badruddin 2014). Long-term data of solar winds and interplanetary plasma/field parameters is available via NASA OMNIWeb online interface (https://omniweb.gsfc.nasa.gov/form/dx1.html/). In this study, solar winds and interplanetary plasma/field parameters, solar wind speed (V (km/s)), the magnitude of magnetic field (B (nT)), north–south component (Bz (nT)) and electric field (Ey (mV/m)) have been analyzed during the passage of HSSs from 1963 to 2016. For this purpose, hourly data of geomagnetic parameters is used to perform the statistical analysis. A correlation analysis is performed among plasma field parameters and geomagnetic activity during the passage of HSSs. Based on the D_{st} index, the solar storms are classified into four groups as weak (-50 nT $< D_{st} < -30$ nT), moderate (-100 nT $< D_{st} < -50$ nT), intense (-200 nT $< D_{st} < -100$ nT) and superstorms ($D_{st} < 200$ nT) (Gonzalez *et al.* 1994). Table 1 represents the list of geomagnetic storms from 1963 to 2016. The effects of geomagnetic disturbances on telecommunications, GPS and navigation systems are also discussed in this paper. Moreover, major geomagnetic storms in the hourly D_{st} index below -100 nT have been selected as a threshold value in a similar way as selected by Tsurutani & Gonzalez (1997).

3. Results

3.1 *Variations of geomagnetic disturbances*

On the basis of the D_{st} index and their strength, geomagnetic disturbances are classified as weak, moderate, intense and superstorms to study the statistical distribution of geomagnetic activity during the years 1963–2016. These ranges have been derived from earlier studies (Gosling *et al.* 1991; Gonzalez *et al.* 1994; Adebesin *et al.* 2013; Mustajab & Badruddin 2017).

Table 2 shows the equations of linear fit and correlation coefficient (R) of plasma/field parameters (V (km/s), B (nT), Bz (nT) and Ey (mV/m)) during the passage of HSSs from 1963 to 2016. In the equation of the linear fit model ($y = mx + c$), x denotes the number of days, m shows the slope of the trend line and y denotes the plasma field parameter. Slope values of all the four HSSs groups depict a decreasing trend of V (km/s) with a maximum negative slope of -42.28, an intercept value of 5,495 and $R = 0.36$ in the superstorms group, whereas the minimum negative slope of -0.06, an intercept of 4524.7 and $R = 0.11$ was observed in the weak storms group, as shown in Table 2. B (nT) shows a decreasing trend in the weak storms group with a negative slope of -5×10^{-6} and $R = 0.01$. In moderate, intense and superstorms groups, B (nT) shows an increasing trend with a maximum slope of 0.1087, intercept of 18.44 and $R = 0.31$ for the superstorms group. Bz (nT) shows a decreasing trend during all the four groups of solar storms with a maximum negative slope value of -0.0275, an intercept of -6.12 and $R = 0.06$ for the super solar storm group. The highest decreasing trend in Ey (mV/m) is observed during superstorms with a slope value of -6.346, an intercept of 849 and $R = 0.44$.

Table 1. List of geomagnetic storms caused by HSSs from 1963 to 2016.

Years	1963	1964	1965	1966	1967	1968	1969	1970	1971
Weak	11	14	9	88	360	498	247	94	181
Moderate	0	9	3	36	0	160	107	19	96
Intense	0	0	0	6	30	15	32	17	4
Super	0	0	0	0	0	0	6	7	0
Years	1972	1973	1974	1975	1976	1977	1978	1979	1980	1981
Weak	496	544	533	285	395	704	1,171	788	1,293	804
Moderate	82	331	209	56	149	433	537	324	876	539
Intense	2	28	24	0	2	53	62	26	139	77
Super	0	0	1	0	0	6	1	6	7	10
Years	1982	1983	1984	1985	1986	1987	1988	1989	1990
Weak	804	426	285	267	237	331	531	604	460
Moderate	539	184	100	47	132	66	209	515	276
Intense	77	7	3	4	25	0	322	79	64
Super	10	0	0	0	0	0	0	1	0
Years	1991	1992	1993	1994	1995	1996	1997	1998	1999
Weak	543	425	354	585	1,198	426	644	884	954
Moderate	576	113	550	241	550	25	234	418	368
Intense	9	38	5	20	23	2	23	109	48
Super	4	0	0	0	0	0	0	2	3
Years	2000	2001	2002	2003	2004	2005	2006	2007	2008
Weak	2,106	830	1,297	1,770	612	768	472	164	183
Moderate	472	442	792	451	242	401	85	17	12
Intense	132	170	1,199	44	95	44	12	0	0
Super	15	28	0	10	19	3	0	0	0
Years	2009	2010	2011	2012	2013	2014	2015	2016	TOTAL
Weak	34	185	403	580	434	344	781	40	28,964
Moderate	15	98	156	327	156	104	396	18	12,835
Intense	0	0	14	58	9	2	54	2	2,856
Super	0	0	0	0	0	0	6	0	135

3.2 *Analysis of yearly average D_{st} index*

D_{st} is used to monitor the magnetic storms level globally and it is the standard measure of ring current activity. Figure 1 represents the time series of average D_{st} from 1963 to 2016. The average positive highest $D_{st} = 2.2887$ nT was observed in 1965, whereas the negative highest $D_{st} = -30.349$ nT is observed in 1991 during the study period. D_{st} shows a decreasing trend during the study period with a slope of -0.004, an intercept of -16.756 and $R^2 = 0.0001$. The intensity of geomagnetic disturbances varies significantly, as shown in Figure 1.

3.3 *Analysis of yearly average Bz (nT)*

Figure 2 shows the average variations of the Bz component of the magnetic field from 1963 to 2016. The positive and negative peak values of the Bz component are 0.4028 and -0.9872 nT, respectively. The slope value of 0.0027 shows an increasing trend of Bz (nT) from 1963 to 2016 with an intercept of -0.0665 and $R^2 = 0.0276$. The orientation relative to the Earth's magnetic field decides the geomagnetic activity around the Earth and its effects on the technological system such as telegraph system, radar system and satellites. If the Bz component of HSSs is directed northward relative to the Earth's geographic north pole, then the inter-planetary magnetic field lines will be oriented in the same way as the Earth's magnetic field lines. Consequently, the interaction between the HSSs magnetic field lines and the Earth's magnetic field lines becomes the minimum. Thus, the technological systems remain unaffected by solar storms. If the Bz component of the inter-planetary magnetic field is directed southward relative to the Earth's North Pole then the inter-planetary magnetic field lines will be oriented in the opposite direction relative to that of the Earth's magnetic field lines.

Table 2. Equation of linear fit model for plasma/field parameters during the passage of HSSs (weak, moderate, intense and superstorms) during 1963–2016.

HSSs' group	No. of events	Equations of linear fit	
		V (km/s)	B (nT)
Weak	28,964	$y = -0.0687x + 4524.7, R = 0.11$	$y = -5 \times 10^{-6}x + 8.086, R = 0.01$
Moderate	12,835	$y = -0.1071x + 4400, R = 0.08$	$y = 3 \times 10^{-5}x + 9.692, R = 0.03$
Intense	2,856	$y = -0.8328x + 4365.3, R = 0.09$	$y = 0.0009x + 13.77, R = 0.07$
Super	135	$y = -42.28x + 5495, R = 0.36$	$y = 0.1087x + 18.44, R = 0.31$
		Bz (nT)	Ey (mV/m)
Weak	28,964	$y = -4 \times 10^{-6}x - 0.567, R = 0.01$	$y = -0.0108x + 594.3, R = 0.17$
Moderate	12,835	$y = -9 \times 10^{-5}x - 1.103, R = 0.06$	$y = -0.0139x + 555.1, R = 0.09$
Intense	2,856	$y = -0.0008x - 3.072, R = 0.04$	$y = -0.154x + 626.2, R = 0.14$
Super	135	$y = -0.0275x - 6.12, R = 0.06$	$y = -6.346x + 849, R = 0.44$

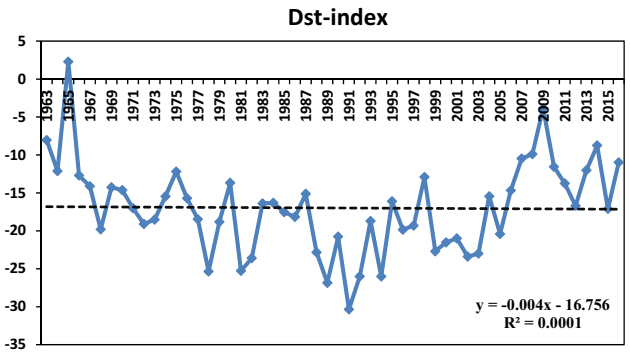

Figure 1. Mean annual variations of the D_{st} index during 1963–2016.

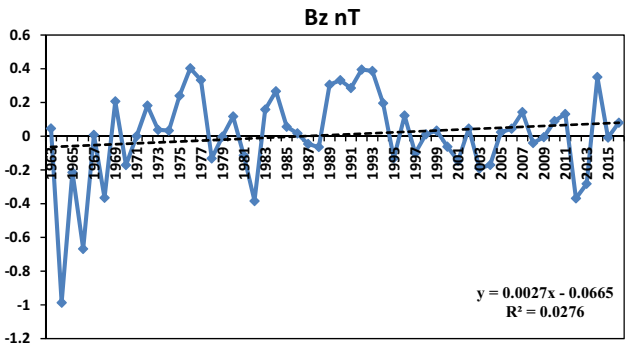

Figure 2. Mean annual variations of Bz (nT) from 1963 to 2016.

3.4 *Analysis of yearly average electric field*

Figure 3 shows the average variations of Ey during the period of 1963–2016. The inter-planetary electric field is an important parameter for the development of large-scale geomagnetic storms. It is observed that the maximum value of Ey raised before the main phase of

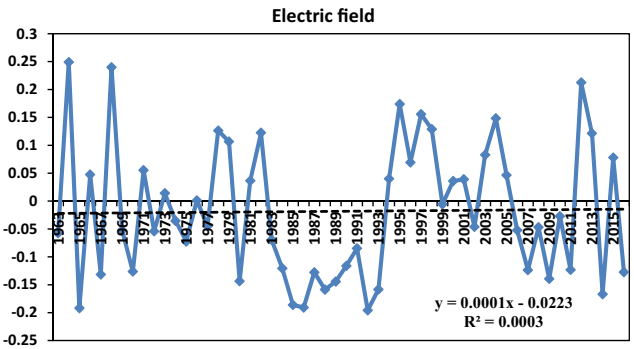

Figure 3. Mean annual variations in an electric field (Ey) during 1963–2016.

geomagnetic storms helps to identify the intensity of the storms (Rathor *et al.* 2014). The energetic protons and ions whose energies lie in between ∼20 and 200 keV suffers a westward drift because of the inclination and the curvature of the geomagnetic field. This westward drift of energetic protons and ions creates a ring current that generates an electric field. The positive slope value of 0.0001 represents an increasing trend of Ey during the study period.

3.5 *Analysis of yearly average* $K_p * 10$ *index*

The time series of the $K_p * 10$ index is shown in Figure 4. K_p is an outstanding indicator of disturbances in the Earth's magnetic field and is used to provide information about the auroral activity i.e., northern and southern lights. A larger southward Bz component and the minimum D_{st} index value allow more energy transfer from interplanetary magnetic field lines into the Earth's magnetosphere resulting in enhanced auroral activities. The slope of −0.0949 shows a

decreasing trend of the $K_p * 10$ index from 1963 to 2016. The average minimum value of $K_p * 10$ was found to be 0.035 nT in the year 2000, whereas the average maximum value of $K_p * 10$ was found to be 32.33 nT in 1994. The variations in the D_{st} index, $K_p * 10$ index, *Ey* and sunspot numbers from 1963 to 2016 are shown in Figure 5.

4. Correlation analysis of peak D_{st} with peak *Ey* (mV/m), *V* (km/s), K_p*10 (nT), *B* (nT) and *Bz* (nT)

The relationship between the peak values of D_{st} and the plasma/field parameters (*E* (mV/m), *V* (km/s), *B* (nT), *Bz* (nT) and $K_p * 10$) from 1963 to 2016 is shown in Figure 6. The linear regression equation and value of *R* for all the parameters are given in Figure 6. The value of *R* among the peak *E* (mV/m) *vs.* D_{st}, *V* (km/s) *vs.* D_{st}, *B* (nT) *vs.* D_{st}, *Bz* (nT) *vs.* D_{st} and $K_p * 10$ *vs.* D_{st} is found to be 0.42, 0.14, 0.51, 0.37 and 0.54, respectively. It is clear from these results that the peak values of D_{st} are well correlated with *E* (mV/m), *Bz* (nT), *B* (nT) and $K_p * 10$, whereas D_{st} is

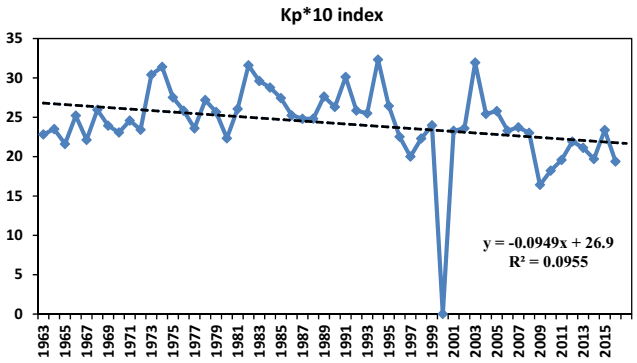

Figure 4. Mean annual variation in $K_p * 10$ index during 1963–2016.

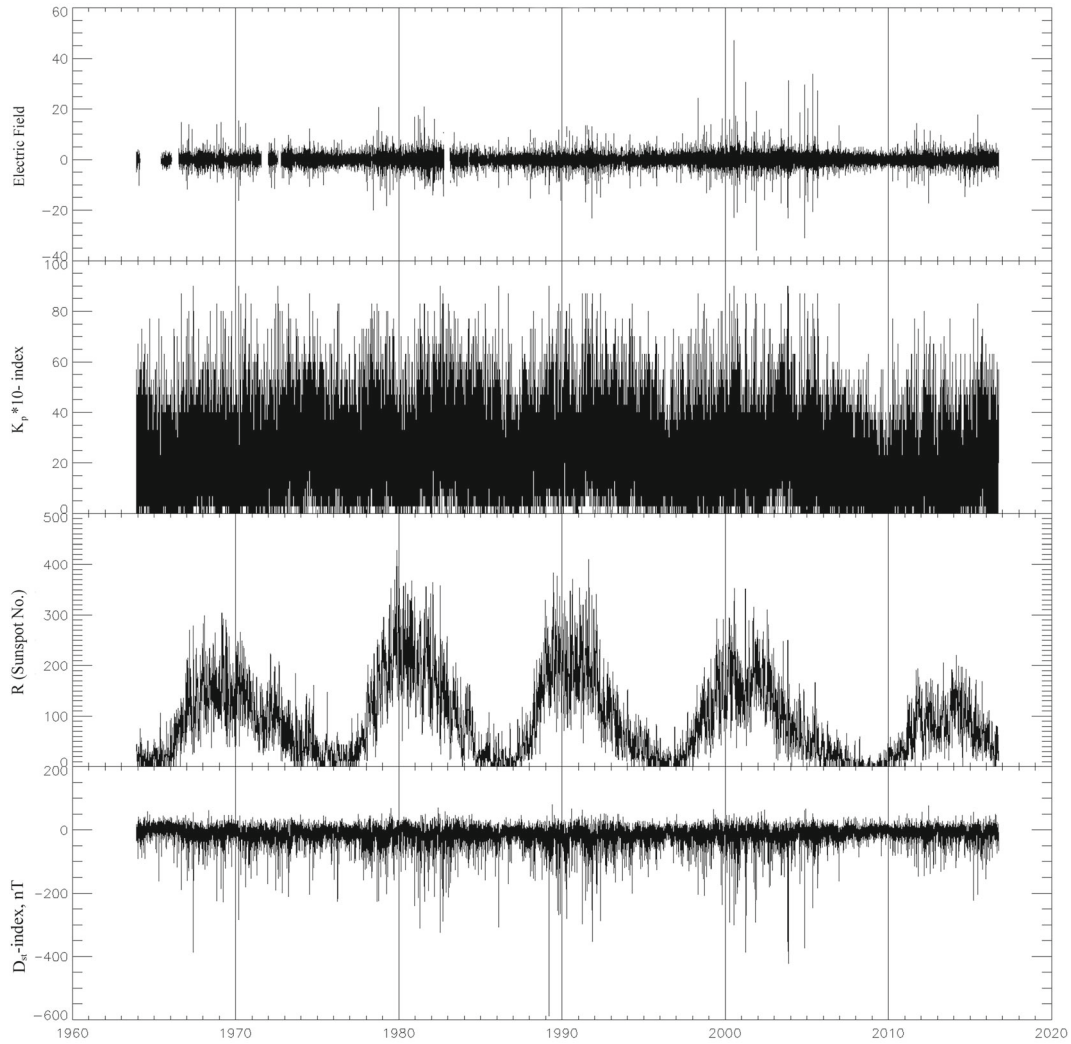

Figure 5. The variations in the D_{st} index, sunspot numbers, $K_p * 10$ index and electric field from 1963 to 2016.

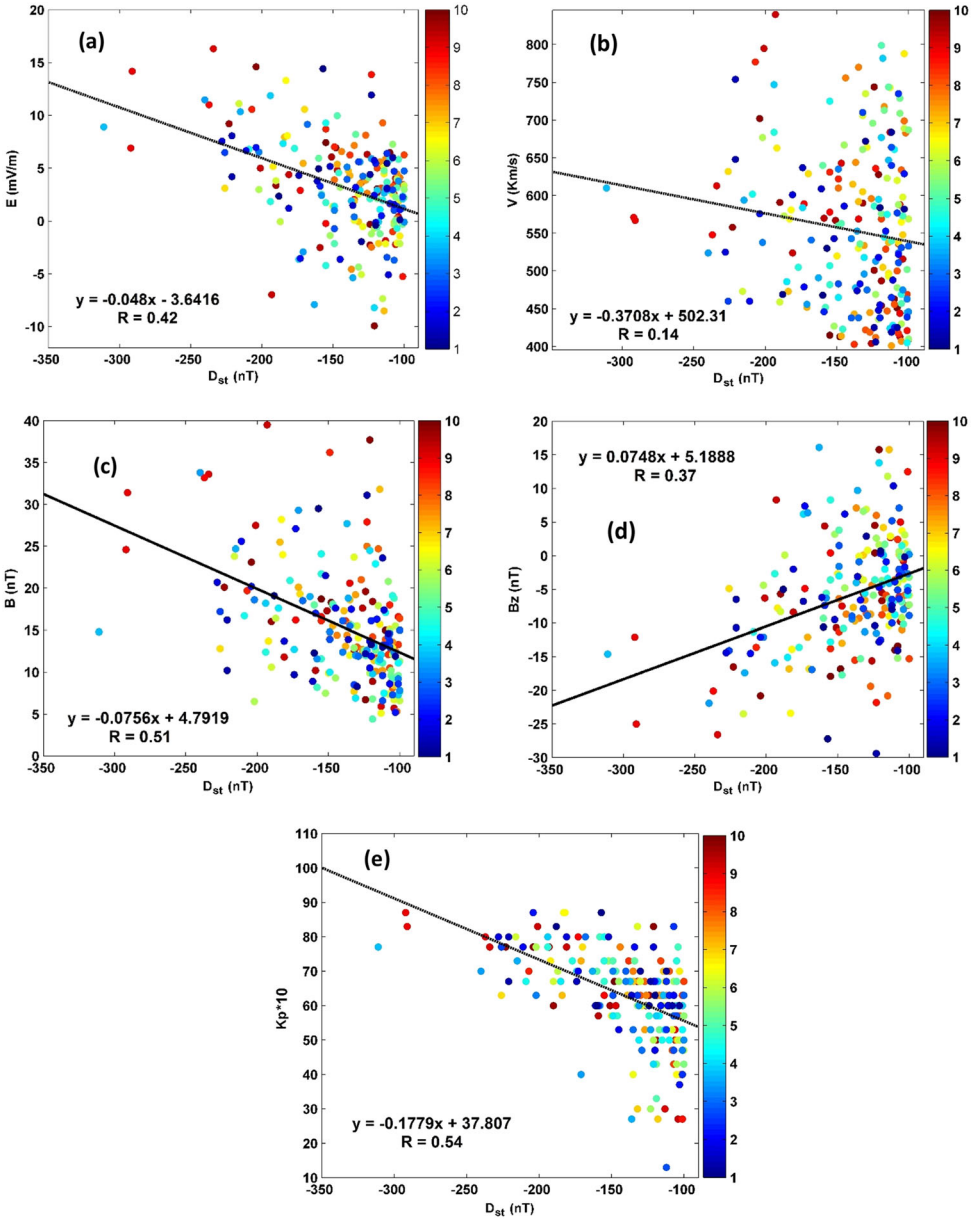

Figure 6. Relationship between peak D_{st} values from 1963 to 2016. (a) E (mV/m) *vs.* D_{st}, (b) V (km/s) *vs.* D_{st}, (c) B (nT) *vs.* D_{st}, (d) Bz (nT) *vs.* D_{st} and (e) $K_p * 10$ *vs.* D_{st}.

moderately correlated with V (km/s). The highest negative slope value of -0.3708 and the intercept of 502.3 are observed between V (km/s) and D_{st}, whereas the lowest negative slope value of -0.048 is observed between E (mV/m) and D_{st}.

5. Effects of the geomagnetic disturbances on telecommunications

The geomagnetic storms create problems for telecommunication networks (McManus *et al.* 2011), pipelines, satellites and radars. Solar flares treat computers and networks by inducting electricity into wires and equipment, and also disturb the radio/wireless communication networks. In the early years, the energy induced by flares might affect the computer wires and telephone switches. The flares interrupt the noise and make communication difficult. The solar storm continues to affect the optical fiber cables and submarine cables, because of induced voltage produced by geomagnetic turbulences (due to the solar storms). Auroras are caused by solar flares erupting from the sun, which can also affect the satellite components and grid stations, and upsets the

Table 3. Historical events of geomagnetic disturbances and their effects on telecommunication.

Event date	Geomagnetic disturbances and their effects
October 2003	In October 2003, a series of solar storms collectively called the "Halloween" caused surges that threatened the southern Sweden power grid. The communication networks were also disturbed when the storm reached its peak value (Pulkkinen *et al.* 2005)
June 15, 2000	The disturbances in telecommunications in China were caused by solar storms on June 2, 2000 (Telecom Services China). There was also a 17-hours' shortwave effect on China Radio Service on June 9. The solar disturbances also affect satellite communications and navigation systems (Long 2000)
March 1989	Fiber-optic cables are used to transfer the signals and repeaters are used to carry the power with the help of conductors. Due to the occurrence of storms, high voltages were observed on the power cables (Space Weather Canada 2009)
February 10, 1958	Transatlantic communication from Clarenville Newfoundland, to Oban, Scotland proceeded as alternate faint whispers as the natural voltage acted contrary to the cable voltage (Space Weather Canada 2009)
March 24, 1940	A voltage of $\sim$500 V affects the phone communications in the United States, whereas in Sweden, the magnetic storms caused arcing in the carbon protectors (Space Weather Canada 2009)
February 19, 1852	Bain's chemical telegraphs are used for the preparation of papers. A chemical reaction left a mark on the paper by the current produced from a stylus. The current increased so much that it sets fire to the paper (Space Weather Canada 2009)
September 1851	In New England, the solar storm occurred and took control of all the telegraph lines and stopped all kinds of businesses during its period (Prescott 1860)
November 17, 1848	The strength of geomagnetic disturbances was witnessed by a man named Matteucci in the electric telegraphs of Italy. The soft iron armatures in the electric telegraph among Florence and Pisa remained to their electro-magnets as if the latter was fully magnetized and without the currents in the battery (Norton 2007)
November 17, 1848	The needle of the electric telegraph moved to the same side even with additional force witnessed by a man named Highton in England (Norton 2007)
April 14, 1779	Benjamin Franklin had wholehearted interest in the observations of solar storms (i.e., Aurora Borealis). He defined that the shifting of lights to a concentration of charges in the polar regions is strengthened by the moisture. He explained that this enhanced charging caused an electrical brightness in the air (Library of Congress 2006)

navigation systems. Some of the events mentioned in Table 3 occurred in the past years due to geomagnetic storms.

6. Conclusions

In this study, the passage of HSSs from 1963 to 2016 has been investigated using solar wind and plasma/field inter-planetary datasets. The results obtained from statistical analyses of plasma/field parameters and geomagnetic activity in the course of HSSs are given below.

Ey was found to be negative during the periods of four HSS groups. The parameters *B* (nT) and *V* (km/s) were opposite of each other during the intense storm disturbances. During the moderate storms, the *Bz* component was found to be negative, whereas *B* (nT) was found to be positive. It was observed that when the D_{st} index increases, *Ey* decreases and vice versa, and these variations changed with the energetics of the storms. It was also observed that variations in *B* (nT) and relative to a D_{st} index occurred oppositely. The D_{st} index best correlates with the $K_p * 10$ index with the highest value of $R = 0.54$. The value of *R* was found to be 0.51 between D_{st} and *B* (nT) during the passage of HSSs. Annual time-series analysis of D_{st} and $K_p * 10$ indices showed a decreasing trend, whereas *Bz* (nT) and *Ey* (mV/m) showed an increasing trend throughout the study period. The slope value of *V* (km/s) showed a decreasing trend with the highest negative slope of -42.28, an intercept of 5,495 and $R = 0.36$ in the superstorms group. The total amount of the energy of the ring current particles was responsible for the reduction of the D_{st} index. The mean annual highest value of the $K_p * 10$ index was 32.33 nT in the year 1994. During intense super-storms, energy penetrating the ionosphere increases,

which in turn increases the value of the K_p index resulting in early warning of stunning auroras i.e., northern and southern lights.

Acknowledgments

The author acknowledged the use of the OMNIWeb database of National Aeronautic and Space Administration/Goddard Space Flight Center (https://omniweb.gsfc.nasa.gov/form/dx1.html/) (NASA/GSFC) for the plasma field parameters for the statistical distribution and the behavior of the geomagnetic disturbances.

References

Adebesin B. O., Ikubanni S. O., Kayode J. S. *et al*. 2013, Afr. Rev. Phys. 8, 19
Akasofu S. I. 1983, Space Sci. Rev. 34, 173
Alves M. V., Echer E., Gonzalez W. D. 2006, J. Geophys. Res., 111, A07S05
Arnoldy R. L. 1971, J. Geophys. Res. 76, 5189
Badruddin B., 1996, Astrophys. Space Sci., 246, 171
Badruddin B., Kumar A. 2015, Sol. Phys. 290, 1271
Badruddin B., Falak Z. 2016, Astrophys. Space Sci. 361, 253
Badruddin B., Kumar A. 2016, Sol. Phys. 291, 559
Bisoi S. K., Chakrabarty D., Janardhan P. *et al*. 2016, J. Geophys. Res. 121, 3882
Bothmer V., Zhukov A. 2007, Space Weather Phys. Effects, 438. ISBN 3540239073
Cho I.-H., Kwak Y.-S., Marubashi K. *et al*. 2012, Adv. Space Res. 50, 777
Dessler A. J., Parker E. N. 1959, J. Geophys. Res. 64, 12
Garton T. M. *et al*. 2018, Astrophys. J. Lett. 869, 1
Gonzalez W. D., Gonzalez A. L. C., Tsurutani B. T. 1990, Planet. Space Sci. 38, 181
Gonzalez W. D., Joselyn J. A., Kamide Y. *et al*. 1994, J. Geophys. Res. 99, 5771
Gosling J. T., McComas D. J., Phillips J. L. *et al*. 1991, J. Geophys. Res. 96, 7831
Gupta V., Badruddin B. 2009, Space Sci. 321, 195
Gupta V., Badruddin B. 2010, Sol. Phys. 264, 165
Intriligator D. I. 1973, WDCA Sol. Terr. Phys., Report UAG-27
Kane R. P. 2007, Adv. Space Res. 39, 1890
Kavanagh A., Denton M. 2007, Astronomy Geophys., 48, 6.24
Krieger A. S., Timothy A. F., Roelof E. C. 1973, Sol. Phys. 29, 505
Kumar A., Badruddin B. 2014, Sol. Phys., 289
Lei J., Thayer J. P., Forbes J. M., Sutton E. K. 2008, AGU Fall Meeting Abstracts, A3
Library of Congress 2006, Library of Congress, Exhibitions, American Treasures
Lindblad B. A., Lundstedt H., Larsson B. 1989, Sol. Phys. 120, 145
Loewe C. A., Prölss G. W. 1997, J. Geophys. Res. 102, 14209
Long W. 2000, Solar storms impact China's telecom services, Space-Daily. http://www.spacedaily.com/news/. Accessed Nov 2009
Maris O., Maris G., 2005, Adv. Space Res. 35, 2129
McManus D. J., Carr H. H., Adams B. M. 2011, Effects Geomagn. Disturbances 5, 3
Menvielle M., Berthelier A. 1991, Rev. Geophys., 29, 415
Mustajab F., Badruddin B. 2011, Space Sci. 82, 43
Mustajab F., Badruddin B. 2013, Space Sci. 82, 43
Mustajab F., Badruddin B. 2017, Adv. Spc. Res., 6
Norton P. 2007, The Aurora Borealis and the Telegraph (http://www.rainbowriderstradingpost.com/article1.html)
Ogunjabi O. *et al*. 2014, Adv. Space Res. 54, 1732
Ovidiu M., Georgeta M. 2005, Adv. Space Res. 35, 2129
Parker E. N. 1963, Interplanetary Dynamical Processes, vol. 8 of Interscience Monographs and Texts in Physics and Astronomy, Interscience Publishers, New York, USA
Prescott G. B. 1860, United States Early Radio History—Telegraph, History, Theory and Practice of the Electric Telegraph, 318
Pulkkinen A., Lindahi S., Viljanen A. *et al.* 2005, Space. Weather., 3, S08C03
Rathor B., Gupta C. D., Parashar K. K. 2014, Int. J. Geosci. 5, 1602
Richardson I. G. 2018, Living Rev. Solar Phys. 15, 1
Sckopke N. *et al*. 1966, J. Geophys. Res. 77, 13
Snyder C. W., Neugebauer M., Rao U. R. 1963, J. Geophys. Res. 68, 6361
Space Weather Canada 2009, Geomagnetic effects on communication cables
Sugiura M., Chapman S. 1960, Wiss. Gottingen, Math. Phys. Kl
Tsurutani B. T., Gonzalez W. D. 1997, Geophys. Monogr. Ser., vol. 98, AGU, Washington, D.C.
Tu C. Y., Zhou C., Marsch E. *et al*. 2005, Science 308, 519
Vršnak B., Dumbović M., Čalogović J. *et al*. 2017, Sol. Phys. 292, 140
Verbanac G., Vršnak B., Živković S. *et al*. 2001, Astron. Astrophys. 533, 49
Wu C. C., Lepping R. P., Berdichevsky D. B. *et al*. 2017, Space. Weather. 15, 3
Xystouris G., Sigala E., Mavromichalaki H. 2014, Sol. Phys. 289, 995
Yermolaev Y. I., Lodkina I. G., Nikolaeva N. S. *et al*. 2018, J. Atmos. Solar-Terr. Phys. 180, 52
Zhang J., Liemohn M. W., Kozyra J. U. *et al*. 2006, J. Geophys. Res. 111, A01104